Journal of Hazardous Materials 182 (2010) 295–302

Contents lists available at ScienceDirect

Journal of Hazardous Materials

journal homepage: www.elsevier.com/locate/jhazmat

Synthesis, characterization and properties of ethylenediamine-functionalized Fe_3O_4 magnetic polymers for removal of Cr(VI) in wastewater

Zhao Yong-Gang[a,b], Shen Hao-Yu[a,*], Pan Sheng-Dong[a,c], Hu Mei-Qin[a]

[a] Ningbo Institute of Technology, Zhejiang University, Ningbo 315100, China
[b] Ningbo Municipal Center for Disease Control & Prevention, Ningbo 315010, China
[c] College of Science, Zhejiang University, Hangzhou 310027, China

ARTICLE INFO

Article history:
Received 7 April 2010
Received in revised form 5 June 2010
Accepted 8 June 2010
Available online 12 June 2010

Keywords:
Ethylenediamine-functionalized magnetic polymers (EDA-MPs)
Functional monomer
Adsorption
Chromium(VI)
Langmuir isotherm

ABSTRACT

A series of ethylenediamine (EDA)-functionalized magnetic polymers (EDA-MPs) have been prepared *via* suspension polymerization with the usage amount of the functional monomer glycidylmethacrylate (GMA) varied during the suspension polymerization procedure. The EDA-MPs were characterized by transmission electron microscopy (TEM), vibrating sample magnetometer (VSM), X-ray diffractometer (XRD), thermogravimetry and differential thermogravimetry analysis (TG-DTA), Fourier-transformed infrared spectroscopy (FTIR) and elementary analyzer (EA). The adsorption properties of the EDA-MPs for the removal of Cr(VI) in wastewater were deeply studied. The results showed the adsorption efficiency was highly pH dependent and decreased with the increasing of initial concentration of Cr(VI). The adsorption data taken at the optimized condition, *i.e.*, 35 °C and pH of 2.5 were well fitted with the Langmuir isotherm. The maximum adsorption capacities (q_m) of EDA-MPs to Cr(VI) were highly related to the contents of EDA-MPs, *i.e.*, the q_m of EDA-MPs to Cr(VI) calculated from the Langmuir isotherm increased from 32.15 to 61.35 mg g^{-1} with the increasing of the usage amount of GMA. The adsorption kinetic data were modeled by the pseudo-second-order rate equation, and the adsorption of Cr(VI) by all the present EDA-MPs reached equilibrium in 60 min.

1. Introduction

Chromium is a kind of widely used industrial chemical, which is applied in electroplating and metal finishing processes, tanning of leather, pigment and chemical industry, *etc.* [1–3]. Chromium has two main oxidation states, *i.e.*, Cr(III) and Cr(VI), in aqueous systems, in which, Cr(VI) is generally considered to pose great human health risk because it is more toxic, soluble and mobile than Cr(III) [4,5]. Cr(VI) exists mainly in soluble forms of $HCrO_4^-$, $Cr_2O_7^{2-}$, and CrO_4^{2-} in aqueous solution, with $HCrO_4^-$ being predominant at pH below 6.5, while changing to CrO_4^{2-} being predominant at pH above 6.5 [6]. Several Cr(VI) compounds act as carcinogens, mutagens and teratogens in biological systems [7]. A series of in vitro and in vivo studies have demonstrated that Cr(VI) induces an oxidative stress through enhanced production of reactive oxygen species (ROS) leading to genomic DNA damage and oxidative deterioration of lipids and proteins [8,9]. Cr(VI) has become one of the most frequently detected ground water at hazardous waste sites. It has been placed on the top of the priority list of toxic pollutants by the U.S. EPA [1]. Therefore, treatment of industry wastewater containing Cr(VI) prior to discharge is essential.

Conventional techniques such as reduction, reverse osmosis, electrodialysis, ion exchange, and adsorption have been used for removing Cr(VI) from wastewater [3]. The reduction followed by precipitation has some disadvantages, *i.e.*, higher waste treatment equipment costs, significantly higher consumption of reagents, and significantly higher volume of sludge generated [10]. Although reverse osmosis and electrodialysis are superior in recovering Cr(VI), it is difficult to reduce Cr(VI) in the effluent to an acceptable level [3]. As far as ion exchange is concerned, it is an attractive approach in treating the wastewater containing Cr(VI), but ion exchange system is the complexity in regenerating the resin and in recovering pure chromic acid [3].

Relatively, adsorption is a conventional but efficient technique to remove Cr(VI) from wastewater. Many kinds of adsorbents for wastewater treatment have been developed, such as activated carbon [11], activated alumina [12], coated silica gel [13] and treated sawdust [14]. However, difficulties for separation rapidly and effectively after treatment from wastewater have been limited their application. To explore more suitable adsorbents for the purpose has become a new great challenge.

Recently, based on the development of magnetic materials (MMs), Hu, et al. reported a kind of magnetite (γ-Fe_2O_3) used to

* Corresponding author. Tel.: +86 574 88130129.
E-mail address: hyshen@nit.zju.edu.cn (H.-Y. Shen).

0304-3894/$ – see front matter © 2010 Elsevier B.V. All rights reserved.
doi:10.1016/j.jhazmat.2010.06.029

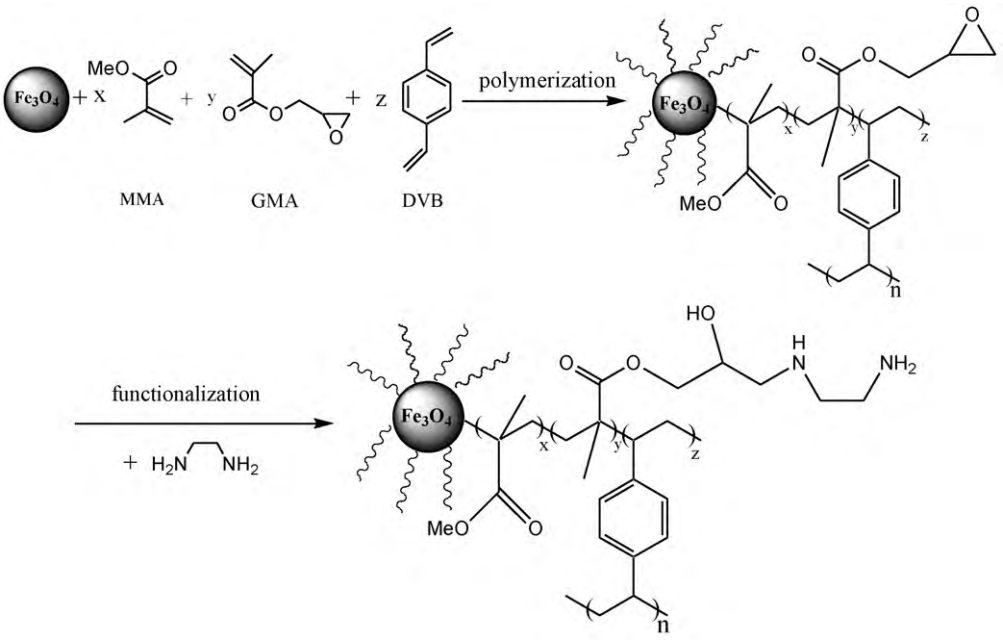

Scheme 1. Amino-functionalization procedure of EDA-MPs.

remove Cr(VI) ion from industrial wastewater, which has superparamagnetic features and convenient separation characteristics under a magnetic field [15]. However, its maximum adsorption capacity was only 17.0 mg g^{-1} [15].

In order to achieve high maximum adsorption capacity, various functional groups, including carboxylate, hydroxyl, sulfate, phosphate, amide and amino groups, have been used to modify the conventional adsorbents [16,17]. Among these adsorbents, amino- functionalized magnetic polymers would be expected to be effective ones for removing heavy metals. Under acidic conditions, amino groups were easier to be protonated and electrostatic attraction happened between $-NH_3^+$ and anions as in Eq. (1) [18]. Here, $-NH_3^+$ and $HCrO_4^-$ were taken as representatives:

$$-NH_3^+ + HCrO_4^- \rightarrow -NH_3^+ \cdots\cdots HCrO_4^- \quad (1)$$

$-NH_3^+$ can also contact with Cl^-, and then ion exchange took place between $HCrO_4^-$ and Cl^- as in Eq. (2) [19]:

$$-NH_3^+Cl^- + HCrO_4^- \rightarrow -NH_3^+HCrO_4^- + Cl^- \quad (2)$$

Recently, Huang et al. reported an amino-functionalized magnetic adsorbent which was prepared by the covalent binding of polyacrylic acid (PAA) on the surface of Fe_3O_4 particles and followed by amino-functionalization with diethylenetriamine (DETA) *via* carbodiimide activation. The maximum adsorption capacity of this adsorbent to Cr(VI) was only 11.24 mg g^{-1} [20], which was slightly lower than that of the magnetite (γ-Fe_2O_3) mentioned above [15]. Thus, although amino-functionalized materials have been proved to be effective ones for removing Cr(VI) from industry wastewater, their adsorption properties would be affected remarkably by the preparation technics.

In this study, a series of novel amino-functionalized magnetic polymers have been synthesized. The paramagnetic Fe_3O_4 was firstly coated with oleic acid. Methyl methacrylate (MMA), divinylbenzen (DVB) and glycidylmethacrylate (GMA) were then co-polymerized *via* the suspension polymerization procedure over the magnetic core to obtain epoxyl-functionalized magnetic polymer. Finally, ethylenediamine was grifted onto the surface of the polymer *via* ring-opening reaction. Thus, the target ethylenediamine-functionalized magnetic polymers were obtained, named as EDA-MPs *infra*. The preparation procedure was illustrated in Scheme 1. The EDA-MPs were characterized by TEM, VSM, XRD, TGA, FTIR and EA.

The objective of this study is to investigate the effect of the usage amount of the functional monomer, *i.e.*, glycidylmethacrylate (GMA) used in the co-polymerization procedure, which would subsequently lead to obtain various EDA-MPs with different amount of amino groups, on the adsorption properties of the EDA-MPs. The effectiveness of the EDA-MPs for the removal of Cr(VI) in wastewater was verified from laboratory batch tests. The optimized adsorption conditions were obtained by intensively investigating the effects of pH value, the initial concentration of Cr(VI), *etc*. The adsorption kinetics and adsorption isotherm were studied. Some promising results were obtained.

2. Experimental

2.1. Materials and reagents

All the necessary chemicals were of analytical grade and were purchased from the Sinopharm Chemical Reagent Co., Ltd. All the dilutions were prepared by ultrapure water.

2.2. Synthesis of EDA-MPs

Fe_3O_4 magnetic particles were prepared according to the reported procedure [21,22] after minor modification. 1.0 g Fe_3O_4 particles was dispersed in 200 mL ethanol under ultrasonication, then 5 mL oleic acid was added dropwisely into the above system under stirring at 80 °C for 1 h. The oleic acid coated Fe_3O_4 particles (OA-M) were isolated in the magnetic field and washed with water and ethanol to remove redundant oleic acid.

The EDA-MPs were prepared by the following steps based on the suspension polymerization and ring-opening reactions.

2.0 g polyglycol was dissolved into 200 mL hot water, followed by adding 4 mL (0.04 mol) methyl methacrylate (MMA) and 2 mL (0.014 mol) divinylbenzen (DVB) and 2 mL (0.013 mol) glycidylmethacrylate (GMA). Then 1.0 g OA-M was dispersed to the above system under ultrasonication. Finally, 1.0 g benzoyl peroxide (BPO) dissolved in 20 mL ethanol was added dropwisely under vigorously stirring. The mixture was continuously reacted at 80 °C for

3 h, yielding M-co-poly(MMA-DVB-GMA) polymer. The resulting M-co-poly(MMA-DVB-GMA) was isolated under magnetic field and washed with water and ethanol to make it free from redundant MMA, DVB and GMA.

1.25 g of the M-co-poly(MMA-DVB-GMA) was dispersed into 50 mL methanol in a 100 mL flask. 7 mL (0.1 mol) of the EDA was added dropwisely under stirring. The flask was then fitted with a water condenser and heated at 80 °C for 8 h. The final amino-functionalized Fe_3O_4 magnetic polymers named as EDA-MPs-2 were isolated under magnetic field and washed with water and methanol to pH value at ~7.0 to remove redundant diamines. The EDA-MPs-2 were dried in a vacuum oven at 60 °C and stored in a sealed bottle for further use.

Other EDA-MPs with different usage amount of glycidylmethacrylate (GMA) (4, 6, 8, 10 mL) were synthesized in a similar way, and named as EDA-MPs-4, EDA-MPs-6, EDA-MPs-8, and EDA-MPs-10, respectively.

2.3. Characterization of EDA-MPs

The morphology and dimensions of the synthesized EDA-MPs were examined by transmission electron microscopy (TEM) (Hitachi H-7650) at 80 kV. Each sample was prepared by placing a very dilute particle suspension onto 400 mesh carbon grids coated with copper film. Magnetic behavior was analyzed by a vibrating sample magnetometer (VSM) (Lake Shore 7410). The structures of EDA-MPs were determined by an X-ray diffractometer (XRD) (Bruker D8 Advance) at ambient temperature. The instrument was equipped with a copper anode generating Cu Kα radiation (λ = 1.5406 Å). Thermogravimetry and differential thermogravimetry analysis (TG-DTA) on a TG 209 F1 instrument at a heating rate of 20 °C min^{-1}, in a nitrogen atmosphere with a flow rate of 20 mL min^{-1}. FTIR spectra were recorded on a Thermo Nicolet (NEXUS-470) FTIR spectrometer. Nitrogen percentage of EDA-MPs was analyzed with an elementary analyzer (EA) (ThermoFisher Flash-1112). Fe_3O_4 percentage was calculated *via* the content of the Fe of EDA-MPs, which was obtained by detection of iron ions using a spectrophotometer (722, Shanghai, China) according to the standard colorimetric method [23]. The concentration of Cr(VI) ions in the aqueous solution was also analyzed with a spectrophotometer (722, Shanghai, China) according to the standard method [24] at a wavelength of 540 nm after acidification of samples with 1N H_2SO_4 and reaction with 1,5-diphenyl carbazide to produce a purple colour complex for colorimetric measurement.

2.4. Adsorption studies

A stock solution of Cr(VI) at concentration of 1000 mg L^{-1} was prepared by dissolving a known quantity of potassium dichromate ($K_2Cr_2O_7$) in ultrapure water. Batch adsorption studies were performed by mixing 0.05 g EDA-MPs with 40 mL $K_2Cr_2O_7$ solution of varying concentration from 10 to 150 mg L^{-1} in a 100 mL stopper conical flask. 1.0 M HCl and 0.5 M NaOH solutions were used for pH adjustment. To investigate the effect of pH, 40 mL of 50 mg L^{-1} Cr(VI) with pH ranging from 2.0 to 9.0 were mixed with 0.05 g EDA-MPs for 24 h to reach equilibrium. When the effect of initial Cr(VI) concentration of the solutions and the usage amount of GMA were investigated, the pH value was 2.5, the usage amount of EDA-MPs was 0.05 g, and the initial Cr(VI) concentration of the solutions was varying from 10 to 150 mg L^{-1}. For the adsorption kinetic studies, under pH value of 2.5, 0.05 g EDA-MPs was added into 40 mL of 50 mg L^{-1} Cr(VI) with contact time ranging from 1 to 120 min, and samples were taken for Cr(VI) concentration measurements at specific time intervals.

2.5. Modeling and analysis of adsorption data

2.5.1. Adsorption model

The equilibrium adsorption capacities, q_e (mg g^{-1}), were determined for each adsorbent by analyzing Cr(VI) concentration before and after the treatment using the equation below:

$$q_e = \frac{(C_0 - C_e)V}{m} \quad (3)$$

where C_0 and C_e are the initial and equilibrium Cr(VI) concentrations in the solution (mg L^{-1}), m is the adsorbent dosage (mg), and V is the volume of the solution (mL), the same hereinafter.

An adsorption isotherm was used to characterize the maximum adsorption capacity of the given adsorbent. Because data on adsorption from a liquid phase were found to fit the Langmuir equation, the adsorption isotherm was tested to validate the Cr(VI) uptake behavior of the adsorbent. The Langmuir model assumes that the adsorption of Cr(VI) occurs on a homogeneous surface by monolayer adsorption without any interaction between the adsorbed ions and is expressed as

$$\frac{C_e}{q_e} = \frac{1}{Kq_m} + \frac{C_e}{q_m} \quad (4)$$

where q_m and K are the Langmuir constants that are related to the maximum adsorption capacity and apparent heat change, respectively.

2.5.2. Kinetic model

The adsorption kinetic data obtained from batch experiments were analyzed using a pseudo-second-order rate equation [25] as

$$\frac{t}{q_t} = \frac{1}{k_2 q_{e.c}^2} + \frac{t}{q_{e.c}} \quad (5)$$

where q_t is the amounts of Cr(VI) adsorbed onto adsorbent any time t (mg g^{-1}) and k_2 is the second-order rate constant at the equilibrium (g mg^{-1} min^{-1}). Thus, by plotting t/q_t against t, the values of k_2 (slope^2/intercept), $q_{e.c}$ (1/slope) and $k_2 q_{e.c}^2$ (the initial adsorption rate (mg g^{-1} min^{-1}), 1/intercept) can be determined graphically from the slope and intercept of the revealed plots.

3. Results and discussion

3.1. Characterization of EDA-MPs

3.1.1. The TEM and XRD analysis of EDA-MPs

The TEM spectra of the EDA-MPs were shown in Fig. 1. It revealed that the diameter of EDA-MPs increased from 300 to 600 nm with the increasing of the usage amount of GMA during the co-polymerization procedure. The XRD of EDA-MPs-4 was taken as a representative for discussion. The XRD patterns of EDA-MPs-4 showed six characteristic peaks of Fe_3O_4 at 2θ of 30.1°, 35.5°, 43.1°, 53.4°, 57.0° and 62.6° corresponding to their indices (2 2 0), (3 1 1), (4 0 0), (4 2 2), (5 1 1) and (4 0 0). It revealed that chemical modification of the magnetic cores did not make significant changes in the phase property of Fe_3O_4 cores.

3.1.2. The VSM and Fe_3O_4 percentage analysis of EDA-MPs

The paramagnetic properties of the EDA-MPs were verified by VSM as shown in Fig. 2. The saturation moments obtained from the hysteresis loop were found to be 12.3, 12.13, 10.51, 8.85 and 5.56 emu g^{-1} for EDA-MPs-2, EDA-MPs-4, EDA-MPs-6, EDA-MPs-8, and EDA-MPs-10, respectively. The results were consistent to the Fe_3O_4 percentage of EDA-MPs, which were found to be 13.3, 10.8, 7.16, 6.39 and 3.3%, respectively. The EDA-MPs were expected to respond well to magnetic fields without any permanent magnetization, making the solid and liquid phases separate easily.

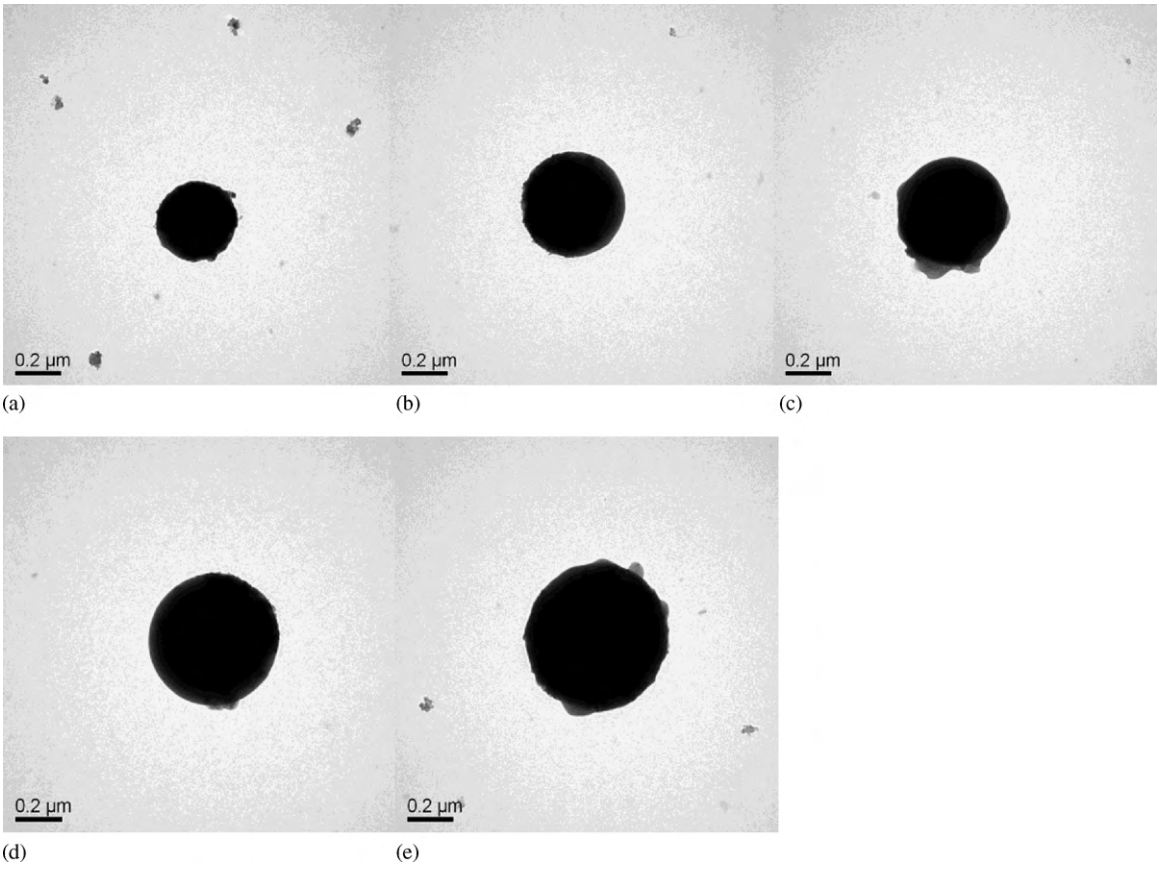

Fig. 1. TEM image of (a) EDA-MPs-2, (b) EDA-MPs-4, (c) EDA-MPs-6, (d) EDA-MPs-8, and (e) EDA-MPs-10.

3.1.3. The TG and EA analysis of EDA-MPs

The TG/DTG analyses of EDA-MPs-10, M-co-poly (MMA-DVB-GMA) and co-poly (MMA-DVB-GMA) were shown in Fig. 3. By comparing the TGA/DTG analyses of EDA-MPs-10 with co-poly (MMA-DVB-GMA), it can be seen that the weight loss (close to 48.7%), beginning at around 370 °C and completing by ~525 °C, could be attributed to the desorption of polymer of the surface layer. While by comparing to M-co-poly (MMA-DVB-GMA), the weight loss (close to 28.6%), beginning at around 290 °C and completing by ~370 °C could be attributed to the desorption of amine groups on the surface and one more weight loss (close to 3.6%), from 525 to 690 °C, could be attributed to the loss of oleic acid (OA). In the case of EDA-MPs-2, EDA-MPs-4, EDA-MPs-6, EDA-MPs-8, and EDA-MPs-10, the results of the TGA/DTG analyses and the nitrogen percentage obtained from EA were listed in Table 1. It can be seen that the weight loss at ~350 °C of the EDA-MPs increased (from ~0% to 28.6%) with the increasing of the usage amount GMA in the preparation procedure, which subsequently resulted in the increasing of amino-groups *via* ring-opening reaction, and eventually leading increasing of the nitrogen percentage (from 1.80% to 3.87%).

Table 1
The TGA and EA analysis of EDA-MPs.

EDA-MPs	TGA						*N* (%)
	T_1 (°C)	TG_1 (%)	T_2 (°C)	TG_2 (%)	T_3 (°C)	TG_3 (%)	
EDA-MPs-2	/	/	430.8	67.08	659.8	9.58	1.80
EDA-MPs-4	341.0	17.91	427.1	56.56	638.2	6.49	2.34
EDA-MPs-6	351.1	21.57	427.9	5386	647.7	5.44	2.88
EDA-MPs-8	348.4	27.32	425.2	50.13	640.4	4.57	3.63
EDA-MPs-10	348.2	28.57	424.5	48.71	631.1	3.6	3.87

3.1.4. The FTIR analysis of EDA-MPs

The IR spectra of OA-M, M-co-poly(MMA-DVB-GMA) and EDA-MPs-8 were shown in Fig. 4. In the IR spectra of OA-M (Fig. 4(a)), the characteristic band of Fe_3O_4 occurs at ~589 cm^{-1}. Other typic bands can be assigned as follows, υ(–OH): ~3446 cm^{-1}, υ(–CH_2, –CH_3): ~2924 cm^{-1}, ~2853 cm^{-1}, υ(C=O): ~1630 cm^{-1} and υ(C=C): ~1429 cm^{-1}. These revealed that the Fe_3O_4 was coated with oleic acid. After co-polymerization, the characteristic absorptions of C=O groups at ~1728 cm^{-1}, C=C groups of benzene at ~1603 cm^{-1}, C–O–C groups at ~1269 and ~1147 cm^{-1} appeared, as shown in Fig. 4(b). After further amino-functionalization, the characteristic peaks of –NH– and –NH_2– groups at ~1638 and ~3422 cm^{-1} appeared, shown in Fig. 4(c). This revealed that the epoxyl- of M-co-poly(MMA-DVB-GMA) had been functionalized successfully with the amino groups *via* ring-opening reaction.

This phenomenon was also observed in the cases of the other four EDA-MPs.

3.2. Effect of pH value on the adsorption properties

40 mL of 50 mg L^{-1} Cr(VI) with pH ranging from 2.0 to 9.0 were mixed with 0.05 g EDA-MPs, and the results were shown in Fig. 5. As shown in Fig. 5, the adsorption efficiency was highly pH dependent. The percentage of uptake of Cr(VI) decreased from 67.3% to 1.73%, 83.2% to 1.63%, and 96.8% to 1.51%, 99.4% to 3.76%, 99.4% to 3.4% gradually with the increasing of pH value from 2.5 to 9.0 for EDA-MPs-2, EDA-MPs-4, EDA-MPs-6, EDA-MPs-8, EDA-MPs-10, respectively.

The dependence of Cr(VI) on the pH can be explained from the perspective of surface chemistry in an aqueous phase. The surfaces of EDA-MPs are generally covered with amino groups that vary in form at different pH levels. Under acidic conditions, amino groups

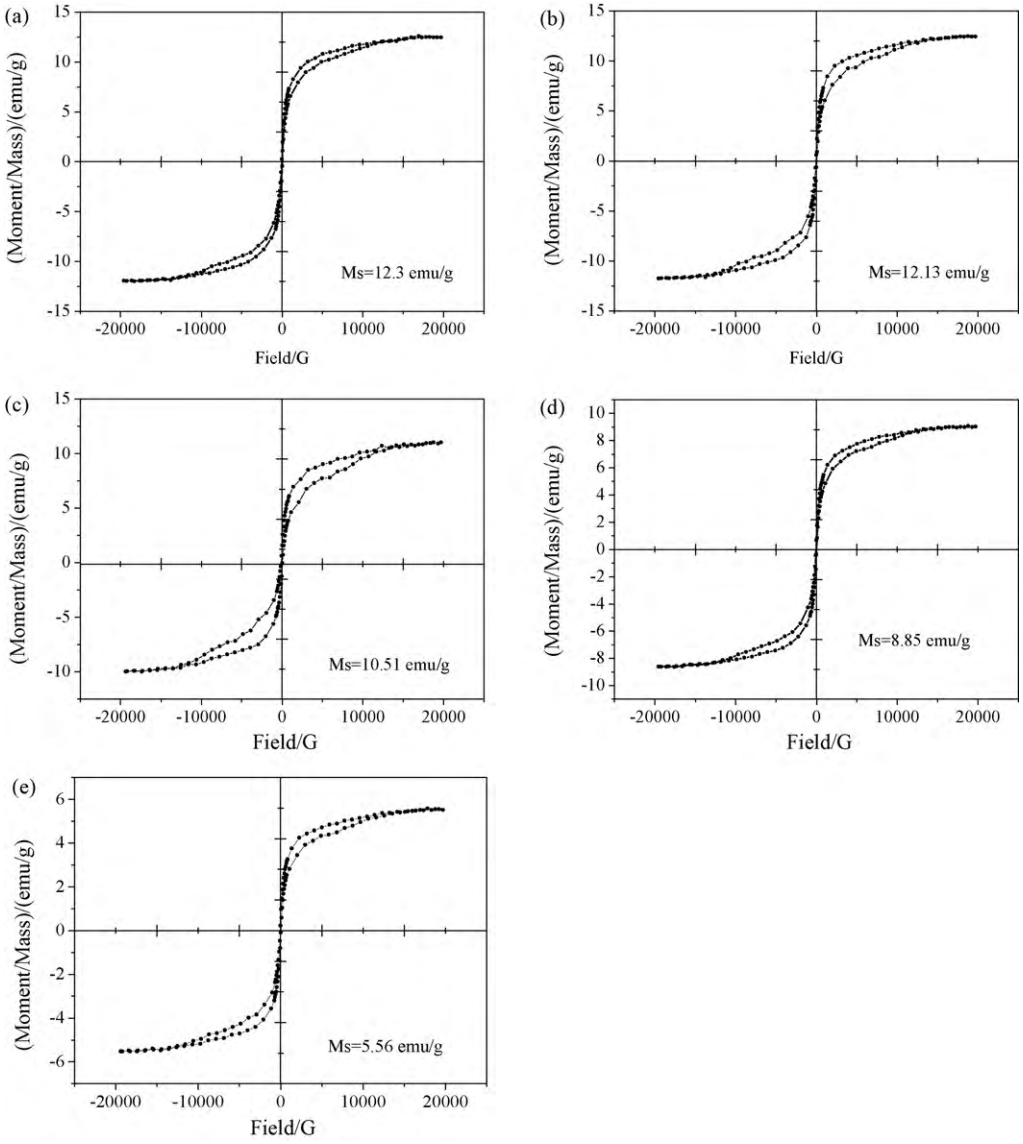

Fig. 2. VSM of (a) EDA-MPs-2, (b) EDA-MPs-4, (c) EDA-MPs-6, (d) EDA-MPs-8, and (e) EDA-MPs-10.

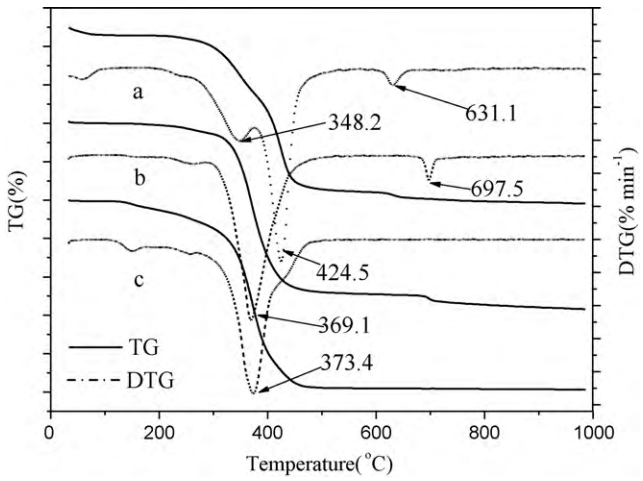

Fig. 3. TGA analysis of (a) EDA-MPs-10, (b) M-co-poly(MMA-DVB-GMA), and (c) co-poly (MMA-DVB-GMA).

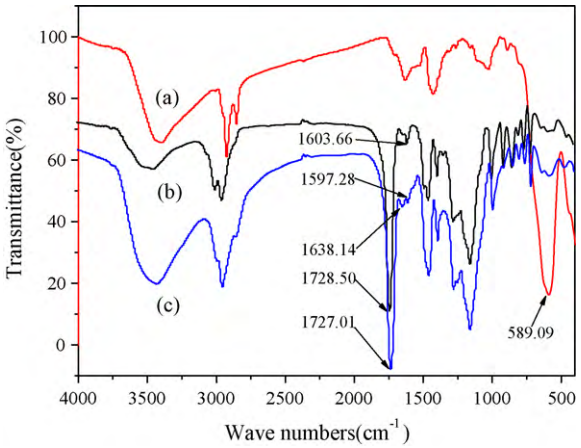

Fig. 4. FTIR adsorption spectra of (a) OA-M, (b) M-co-poly(MMA-DVB-GMA) and (c) EDA-MPs-8.

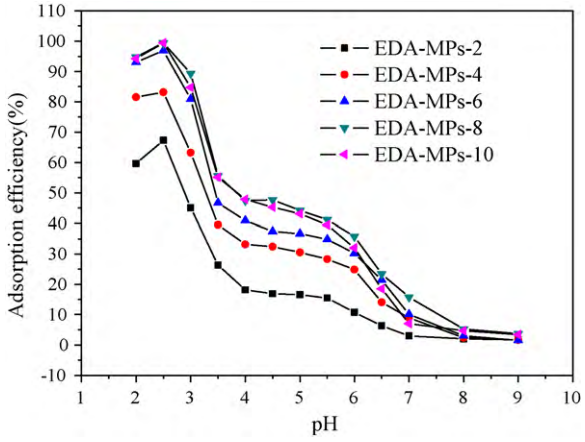

Fig. 5. Effect of pH value on the adsorption of Cr(VI) by EDA-MPs.

were easier to be protonated and electrostatic attraction happened as in Eq. (1), $-NH_3^+$ can also contact with Cl^-, and then ion exchange took place between $HCrO_4^-$ and Cl^- as in Eq. (2). With increasing of the pH value, the concentration of H^+ was decreased, and at the same time the concentration of OH^-, which competed with $HCrO_4^-$, was increased. So the ability of $-NH_2$ to be protonated was weakened, resulting in the decline of removal efficiency.

3.3. Effect of initial concentration on the adsorption properties

40 mL of 50 mg L^{-1} Cr(VI) solution and 0.05 g EDA-MPs were mixed with pH value at 2.5. The effect of initial concentration on the adsorption of Cr(VI) was shown in Fig. 6. Similar curve shapes of all the EDA-MPs were observed. The adsorption efficiencies of Cr(VI) decreased with the increasing of the initial Cr(VI) concentration, while the adsorption capacities increased. This is expected due to the fact that for a fixed adsorbent dosage, the total available adsorption sites are limited thus leading to a decrease in percentage removal of the adsorbate with an increasing of the initial concentration. However, with the increasing of initial concentration of Cr(VI), the adsorption capacities increased before it reached the adsorption equilibrium. In this work, the adsorbate solute equilibrium concentration for EDA-MPs-2, EDA-MPs-4, EDA-MPs-6, EDA-MPs-8, EDA-MPs-10, were 100, 100, 120, 140, 140 mg L^{-1}, while the adsorption capacities were 32.25, 35.57, 48.85, 61.15, 61.69 mg g^{-1}, respectively.

3.4. Effect of the usage amount of GMA

As mentioned above, the adsorption properties of amino-functionalized MPs would be affected remarkably by the preparation technics, the effects of the usage amount of GMA in the polymerization process on the adsorption capacity were deeply investigated in this work. The adsorption behaviors of the EDA-MPs obey Langmuir equation. The adsorption isotherms of EDA-MPs were obtained at temperature of 35 °C and pH value at 2.5 by varying the initial concentration of Cr(VI) from 10 to 150 mg L^{-1}, and the results were shown in Fig. 7. The Langmuir isotherm, parameters and the correlation coefficient of the adsorption data to the equations were listed in Table 2. It can be seen that the Langmuir model effectively described the adsorption data with all $R^2 > 0.99$. Thus, the applicability of monolayer coverage of Cr(VI) on the surface of EDA-MPs was verified. By comparison of q_m, the adsorption capacity of Cr(VI) onto EDA-MPs increased from 32.15 to 61.35 mg g^{-1} with the increasing of the amount of GMA from 2 to 10 mL used for EDA-MPs preparation. As a functional monomer, glycidylmethacrylate (GMA) the more it was used in the polymerization process,

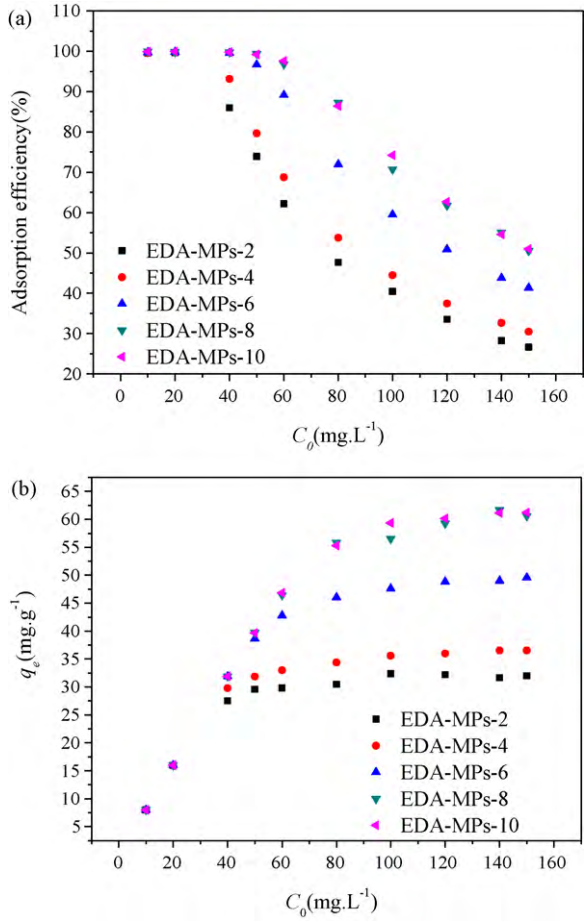

Fig. 6. Effect of initial concentration on the adsorption efficiency (a) and adsorption capacities (b) of Cr(VI) by EDA-MPs.

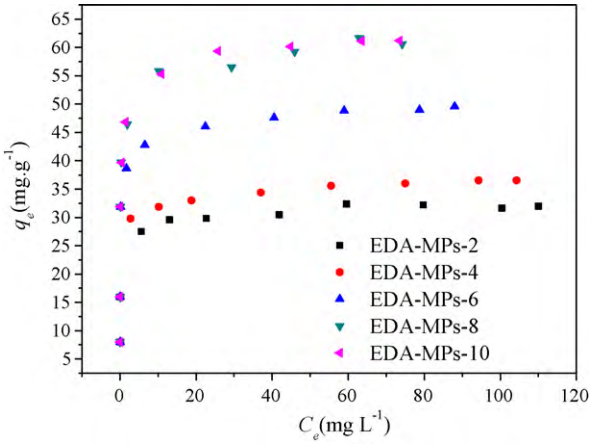

Fig. 7. Langmuir isotherms for Cr(VI) adsorption onto EDA-MPs.

Table 2
The Langmuir isotherms and constants of EDA-MPs.

EDA-MPs	Langmuir isotherms	Langmuir constants		
		K (L mg^{-1})	R^2	q_m (mg g^{-1})
EDA-MPs-2	$C_e/q_e = 0.0311C_e + 0.0251$	1.239	0.9995	32.15
EDA-MPs-4	$C_e/q_e = 0.0273C_e + 0.0305$	0.8951	0.9995	36.63
EDA-MPs-6	$C_e/q_e = 0.0202C_e + 0.0127$	1.591	0.9997	49.5
EDA-MPs-8	$C_e/q_e = 0.0164C_e + 0.0079$	2.076	0.9986	60.98
EDA-MPs-10	$C_e/q_e = 0.0163C_e + 0.0064$	2.547	0.9998	61.35

Table 3
The pseudo-second-order rate equations and constants of EDA-MPs.

EDA-MPs	Pseudo-second-order rate equations	k_2 (g mg^{-1} min^{-1})	q_e (mg g^{-1})	$q_{e.c}$ (mg g^{-1})	$k_2q_e^2$ (mg g^{-1} min^{-1})	R^2
EDA-MPs-2	$t/q_t = 0.0391t + 0.0133$	0.0938	25.4	25.58	75.19	0.9999
EDA-MPs-4	$t/q_t = 0.0358t + 0.0147$	0.0872	27.6	27.93	68.03	0.9999
EDA-MPs-6	$t/q_t = 0.0298t + 0.0142$	0.0625	33.3	33.56	70.42	1
EDA-MPs-8	$t/q_t = 0.0269t + 0.022$	0.0329	36.9	37.17	45.45	0.9999
EDA-MPs-10	$t/q_t = 0.0268t + 0.0206$	0.0349	37.0	37.31	48.54	1

Table 4
Adsorption capacities of various adsorbents for Cr(VI).

Adsorbents	Equilibrium time (min)	pH	q_m (mg g^{-1})	Ref.
EDA-MPs-2	5	2.5	32.15	This work
EDA-MPs-4	10	2.5	36.63	This work
EDA-MPs-6	30	2.5	49.5	This work
EDA-MPs-8	60	2.5	60.98	This work
EDA-MPs-10	60	2.5	61.35	This work
Crosslinked cationic starch maleates	20	4.0	35.71	[26]
Wheat bran	1440	2.1	35	[27]
Modified $MnFe_2O_4$	5	2.0	31.55	[28]
Iron humate	r.t.	3.9–4.6	20	[29]
Maghemite nanoparticles	15	2.0	19.2	[10]
Poly(GMA-co-MMA)-ED	120	2.0	22.9[a]	[30]
Green algae Spirogyra species	120	2.0	14.7	[31]
Chlamydomonas reinhardtii	120	2.0	18.2	[32]
Lignin	>600	~3.0	5.64	[33]

[a] Calculated from literature (reported as 0.441 mol L^{-1}).

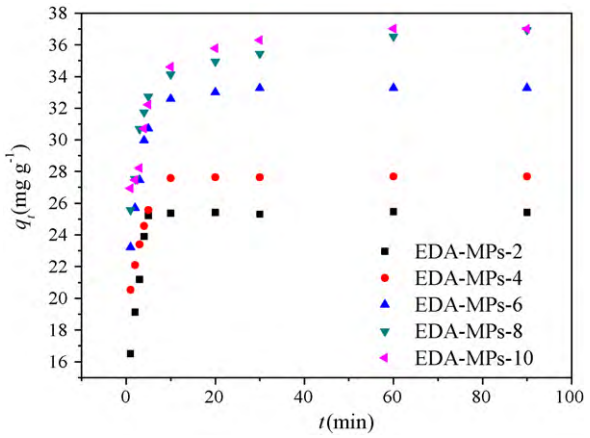

Fig. 8. Kinetic studies on the adsorption of Cr(VI) by EDA-MPs.

the more epoxyl-groups in the epoxyl-MPs would be obtained, which would subsequently lead to more amino groups binded onto the surface of the Fe_3O_4 cores *via* ring-opening reaction. Eventually, higher maximum adsorption capacities can be achieved. These results were consistent with the findings in the TGA analysis above and the results of EA analysis as described in Table 1 for all of the EDA-MPs. The values of q_m increased from 32.15 to 61.35 mg g^{-1} with the increasing of nitrogen percentage from 1.80% to 3.87% in the EDA-MPs, which indicated that the amino groups played a very important role in the adsorption process of Cr(VI) in aqueous solution.

3.5. Kinetic studies

In order to monitor the adsorption kinetic process, 40 mL of 50 mg L^{-1} Cr(VI) solution were mixed with 0.05 g EDA-MPs at pH value of 2.5, and samples were taken at intervals. The results were shown in Fig. 8. It can be seen that the adsorption rate of each EDA-MPs to Cr(VI) was initially quite high, then gradually reached to an equilibrium in 60 min. The adsorption kinetic data obtained from batch experiments have been analyzed using a pseudo-second-order rate equation. The equations and the values of k_2 and $q_{e.c}$ and the initial adsorption rate ($k_2q_e^2$) calculated from the equations were listed in Table 3. The calculating equilibrium adsorption capacities ($q_{e.c}$) from the pseudo-second-order model (25.58, 27.93, 33.56, 37.17 and 37.31 mg g^{-1}) were close to the experimental q_e (25.4, 27.6, 33.3, 36.9 and 37.0 mg g^{-1}) for EDA-MPs-2, EDA-MPs-4, EDA-MPs-6, EDA-MPs-8 and EDA-MPs-10, respectively. This indicated that this model can be applied to predict the adsorption kinetic and the adsorption capacities of the EDA-MPs adsorbents were proportional to the number of active sites on their surface [25]. Along with the functional groups of amine increased, the number of active sites on their surface increased as well, which resulted in increasing of q_e for EDA-MPs.

3.6. Adsorption properties comparison

The maximum adsorption capacities of EDA-MPs with other adsorbents examined for the removal of Cr(VI) under similar conditions reported in the literature were summarized in Table 4. As shown in Table 4, any of the present EDA-MPs had a much higher maximum adsorption capacity compared to other adsorbents reported in the literature. They are very promising particles for the removal of Cr(VI) in wastewater.

4. Conclusion

From above discussion, following conclusions can be drawn:

(1) A series of core–shell structured EDA-MPs have been synthesized. TEM and XRD analyses revealed that the structure of Fe_3O_4 cores was not changed significantly after copolymerization and amino-functionalization. Although magnetic measurement revealed that the magnetic properties of EDA-MPs was not so strong as pure Fe_3O_4 cores, the EDA-MPs were expected to respond well to magnetic fields without any permanent magnetization, therefore making the solid and liquid phases separate easily. TGA and FTIR analysis indicated the amino-functionalization has been accomplished by the reaction

between the epoxyl-groups of glycidylmethacrylate (GMA) and the amino groups of ethylenediamine (EDA) *via* ring-opening reaction.

(2) The effectiveness of the present EDA-MPs for the removal of Cr(VI) in wastewater were verified from laboratory batch tests. The removal efficiency was highly pH dependent and the optimal adsorption occurred at pH 2.5. The adsorption data for Cr(VI) onto EDA-MPs were well fitted with the Langmuir isotherm, and the maximum adsorption capacity increased with the increasing of the usage amount of the functional agent, *i.e.*, glycidylmethacrylate (GMA).

(3) The adsorption of Cr(VI) by all the present EDA-MPs reached equilibrium in 60 min. The data of adsorption kinetics obeyed pseudo-second-order rate mechanism well with an initial adsorption rate of 75.19, 68.03, 70.42, 45.45 and 48.54 $mg\,g^{-1}\,min^{-1}$ for EDA-MPs-2, EDA-MPs-4, EDA-MPs-6, EDA-MPs-8 and EDA-MPs-10, respectively.

Acknowledgments

We would like to thank the Ministry-of-Education Key Laboratory for the Synthesis and Application of Organic Functional Molecules (2007-KL-2007), the Zhejiang Science and Technology Bureau (2007F0045) and the Ningbo Science and Technology Bureau (2009A610002) for the financial support.

References

[1] J.J. Testa, M.A. Grela, M.I. Litter, Heterogeneous photocatalytic reduction of chromium(VI) over TiO_2 particles in the presence of oxalate: involvement of Cr(V) species, Environ. Sci. Technol. 38 (2004) 1589–1594.
[2] K.J. Sreeram, J.R. Rao, R. Sundaram, B.U. Nair, T. Ramasami, Semi-continuous recovery of chromium from waste water, Green Chem. 2 (2000) 37–41.
[3] Y.Q. Xing, X.M. Chen, D.H. Wang, Electrically regenerated ion exchange for removal and recovery of Cr(VI) from wastewater, Environ. Sci. Technol. 41 (2007) 1439–1443.
[4] H.J. Park, L.L. Tavlarides, Adsorption of chromium(VI) from aqueous solutions using an imidazole functionalized adsorbent, Ind. Eng. Chem. Res. 47 (2008) 3401–3409.
[5] R. Ansari, N.K. Fahim, Application of polypyrrole coated on wood sawdust for removal of Cr(VI) ion from aqueous solutions, React. Funct. Polym. 67 (2007) 367–374.
[6] J.M. Sun, F. Li, J.C. Huang, Optimum pH for Cr^{6+} Co-removal with Mixed Cu^{2+}, Zn^{2+}, and Ni^{2+} precipitation, Ind. Eng. Chem. Res. 45 (2006) 1557–1562.
[7] C.C. Liu, M.K. Wang, C.S. Chiou, Y.S. Li, Y.A. Lin, S.S. Huang, Chromium removal and sorption mechanism from aqueous solutions by wine processing waste sludge, Ind. Eng. Chem. Res. 45 (2006) 8891–8899.
[8] R.P. Farrell, R.J. Judd, P.A. Lay, N.E. Dixon, R.S.U. Baker, A.M. Bonin, Chromium(V)-induced cleavage of DNA: are chromium(V) complexes the active carcinogens in chromium(VI)-induced cancers? Chem. Res. Toxicol. 2 (1989) 227–229.
[9] S. Memon, M. Tabakci, D.M. Roundhill, M. Yilmaz, Synthesis and evaluation of the Cr(VI) extraction ability of amino/nitrile calix[4]arenes immobilized onto a polymeric backbone, React. Funct. Polym. 66 (2006) 1342–1349.
[10] J. Hu, G.H. Chen, I.M.C. Lo, Removal and recovery of Cr(VI) from wastewater by maghemite nanoparticles, Water Res. 39 (2005) 4528–4536.
[11] P.C. Manuel, M.M. Jose, T.M. Rosa, Chromium(VI) removal with activated carbons, Water Res. 29 (1995) 2174–2180.
[12] N.R. Bishnoi, M. Bajaj, N. Sharma, A. Gupta, Adsorption of Cr(VI) on activated rice husk carbon and activated alumina, Bioresour. Technol. 91 (2004) 305–307.
[13] D. Gang, W. Hu, S.K. Banerji, T.E. Clevenger, Modified poly-(4-vinylpyridine) coated silica gel. Fast kinetics of diffusion-controlled sorption of chromium(VI), Ind. Eng. Chem. Res. 40 (2001) 1200–1204.
[14] V.K. Garg, R.K. Gupta, Adsorption of chromium from aqueous solution on treated sawdust, Bioresour. Technol. 92 (2004) 79–81.
[15] J. Hu, G.H. Chen, I.M.C. Lo, Selective removal of heavy metals from industrial wastewater using maghemite nanoparticle: performance and mechanisms, J. Environ. Eng. 132 (2006) 709–715.
[16] Y. Sag, Biosorption of heavy metals by fungal biomass and modeling of fungal biosorption: a review, Sep. Purif. Methods 30 (2001) 1–48.
[17] R. Gulati, R.K. Saxena, R. Gupta, Fermentation waste of Aspergillus terreus: a potential copper biosorbent, World J. Microbiol. Biotechnol. 18 (2002) 397–401.
[18] S.B. Deng, Y.P. Ting, Polyethylenimine-modified fungal biomass as a high-capacity biosorbent for Cr(VI) anions: sorption capacity and uptake mechanisms, Environ. Sci. Technol. 39 (2005) 8490–8496.
[19] P.S. Kulkarni, V. Kalyani, V.V. Mahajani, Removal of hexavalent chromium by membrane-based hybrid processes, Ind. Eng. Chem. Res. 46 (2007) 8176–8182.
[20] S.H. Huang, D.H. Chen, Rapid removal of heavy metal cations and anions from aqueous solutions by an amino-functionalized magnetic nano-adsorbent, J. Hazard. Mater. 163 (2009) 174–179.
[21] C. Qus, H.B. Yang, D.W. Ren, Magnetite nanoparticles prepared by precipitation from partially reduced ferric chloride aqueous solutions, J. Colloid Interface Sci. 215 (1999) 190–192.
[22] P. Berger, N.B. Adelman, K.J. Bechman, Preparation and properties of an aqueous ferro fluid, J. Chem. Edu. 76 (1999) 448–943.
[23] B.X. Cai, Y.W. Chen, Basical Chemistry Experiments, Science Press, Beijing, China, 2001.
[24] P.E. Molokwane, K.C. Meli, E.M. Nkhalambayausi-Chirwa, Ethylenediamine grafted poly (glycidylmethacrylate-co-methylmethacrylate) adsorbent for removal of chromate anions, Water Res. 42 (2008) 4538–4548.
[25] Y.M. Ren, M.L. Zhang, D. Zhao, Synthesis and properties of magnetic Cu(II) ion imprinted composite adsorbent for selective removal of copper, Desalination 228 (2008) 135–149.
[26] G.X. Xing, S.F. Zhang, B.Z. Ju, J.Z. Yang, Study on adsorption behavior of crosslinked cationic starch maleate for chromium(VI), Carbohydr. Polym. 66 (2006) 246–251.
[27] L. Dupont, E. Gallon, Removal of hexavalent chromium with a lignocellulosic substrate extracted from wheat bran, Environ. Sci. Technol. 37 (2003) 4235–4241.
[28] J. Hu, I.M.C. Lo, G.H. Chen, Fast removal and recovery of Cr(VI) using surface-modified jacobsite ($MnFe_2O_4$) nanoparticles, Langmuir 21 (2005) 11173–11179.
[29] P. Janoš, V. Hula, P. Bradnová, V. Pilařová, J. Šedlbauer, Reduction and immobilization of hexavalent chromium with coal- and humate-based sorbents, Chemosphere 75 (2009) 732–738.
[30] G. Bayramoglu, M.Y. Arıca, Ethylenediamine grafted poly(glycidylmethacrylate-co -methylmethacrylate) adsorbent for removal of chromate anions, Sep. Purif. Technol. 45 (2005) 192–199.
[31] V.K. Gupta, A.K. Shrivastava, N. Jain, Biosorption of chromium(VI) from aqueous solutions by green algae Spirogyra species, Water Res. 35 (2001) 4079–4085.
[32] M.Y. Arica, İ. Tuzun, E. Yalcın, Ö. İnce, G. Bayramoglu, Utilisation of native, heat and acid-treated microalgae Chlamydomonas reinhardtii preparations for biosorption of Cr(VI) ions, Process Biochem. 40 (2005) 2351–2358.
[33] S.B. Lalvani, A. Hubener, T.S. Wiltowski, Chromium adsorption by lignin, Energy Sources 22 (2000) 45–56.